Synthesis of Ti_3SiC_2-based composites by spark plasma sintering of preceramic papers

E B Kashkarov[1], M S Syrtanov[1], E P Sedanova[1], A S Ivashutenko[1], A M Lider[1] and N Travitzky[1,2]

[1] National Research Tomsk Polytechnic University, 634050 Tomsk, Russia
[2] Friedrich-Alexander-Universität Erlangen-Nürnberg, 91054 Erlangen, Germany

E-mail: egor_kashkarov@mail.ru

Abstract. This paper is devoted to fabrication of Ti_3SiC_2-based ceramic materials from preceramic paper using spark plasma sintering (SPS) method. The synthesis temperature and pressure were 1373-1473 K and 30 MPa, respectively. The phase composition, microstructure and elemental composition were analysed using X-ray diffraction, scanning electron microscopy and energy-dispersive X-ray spectroscopy, respectively. The effect of temperature on the sintering process as well as on the phase and microstructure of the sintered materials was investigated.

1. Introduction

In the last decades much attention has been paid to developing composite ceramic materials based on non-oxide carbon compounds. Among them, the synthesis of MAX-phase ceramics has a great interest due to specifics of its crystalline structure providing unique combination of properties such as high melting temperature, thermal shock resistance, high elastic modulus, oxidation and corrosion resistance, thermal conductivity and mechanical manufacturability. The MAX-phases are a relatively new class of refractory materials described by the formula $M_{n+1}AX_n$, where M– transition metal, A –IIIA-IVA periodic element, X – carbon or nitrogen. Different techniques are implemented to synthesize MAX-phase ceramic materials such as hot isostatic pressing, spark plasma sintering and self-propagating high-temperature synthesis [1, 2].

In the recent years spark plasma sintering is widely used for MAX-phase synthesis due to its great potential for manufacturing single-phase dense materials in relatively short time at considerably lower temperature. Such materials possess superior mechanical properties in comparison with the ones produced by traditional processes of hot isostatic pressing or other sintering techniques [3]. For the first time, Ti_3SiC_2 MAX-phase was synthesized by Zhang et al. using spark plasma sintering of Ti, Si, C powders [4]. This research group obtained the purity of the synthesized product of more than 98%. It has been also shown that the initial powder ratio (Ti, Si and C), powder purity, synthesis temperature and heating rate significantly influences on the forming ceramic composites based on Ti_3SiC_2 [5]. Different approaches were implemented to decrease the synthesis temperature of Ti_3SiC_2 such as addition of trace amount of aluminum [6, 7]. Different compositions and powder mixtures have been used and investigated during SPS. The vast majority of research is aimed at decreasing the synthesis temperature, manufacturing high purity and density composites as well as the properties of synthesized MAX-phase ceramics.

Novel approach based on application of preceramic papers as a feedstock for SPS is suggested in the present research. Preceramic papers are promising materials for manufacturing of complex shaped bodies as well as for the synthesis of graded structures [8–10]. This is due to the possibility to construct multilayer (laminar) structures from preceramic papers with the potential to modify their composition [11]. At the same time, the kinetic processes of MAX-phase synthesis from preceramic papers by SPS remain unstudied. The aim of this research is to fabricate Ti_3SiC_2-based MAX-phase ceramics by spark plasma sintering of Ti_3SiC_2 preceramic papers.

2. Materials and Methods

2.1. Synthesis of Ti_3SiC_2-based ceramics

The preceramic paper sheets with the ceramic filer (Ti_3SiC_2 powder) were fabricated by a laboratory dynamic hand-sheet former (Dynamic hand-sheet former D7, Sumet Systems GmbH, Germany). During paper processing the aqueous feedstock suspension was sprayed on a perforated rotating wire. The concentration of the fibers in the water-based solution was set to 1.2 wt.%. The concentration of the ceramic filler in preceramic papers was set to 90 wt.%. After dewatering paper sheets with a dimension of 94×25×0.05 cm³ were dried at 110 °C for 15 min, and then calendered.

The final preceramic paper was cut into the round sheets of 20 mm in diameter. The spark plasma sintering of the preceramic paper sheets was conducted using HPD25 (FCT Systeme GmbH, Germany). The stack of 12 layers of preceramic paper is placed between two graphite punches in a graphite die. A graphite foil is introduced at the punch/sample interface to ensure a good electrical contact. A constant pressure of 30 MPa is applied during the whole sintering cycle. The temperature is measured during sintering using a pyrometer. The composition of the preceramic paper sheets and SPS parameters are shown in Table 1.

Table 1. The composition of preceramic paper and SPS parameters.

Paper composition		Sintering parameters	
Cellulose fibers	13.35 %	Temperature	1373–1473 K
Ti_3SiC_2 powder	164.7 %	Heating rate	180 K/min
Cationic starch	1.8 %	Holding time	10 min
Anionic starch	1.8 %	Pressure	30 MPa
Retention aid	1.4 %	Atmosphere	Vacuum

2.2. Characterization

The phase composition was analyzed by X-ray diffraction (CuK_α radiation) using XRD 7000S diffractometer (Shimadzu, Japan) equipped with 1280-channel high-speed detector OneSight. The acceleration voltage and current were 40 kV and 30 mA, respectively. Diffraction patterns were recorded at following parameters: 2θ range – 5–80°; scan speed – 10.0°/min; sampling pitch – 0.0143°; exposure time – 21.49 s. The diffraction data was analyzed using Sleve+ program and ICDD PDF-4+ database. The following cards were used as the reference: Ti_3SiC_2 (#00-059-0189), TiC (#00-031-1400), TiSi (#04-008-9158), $TiSi_2$ (#03-065-2522). The microstructure and chemical composition were analyzed by scanning electron microscopy (SEM) using Vega 3 (Tescan, Brno, Czech Republic) equipped with energy-dispersive X-ray spectroscopy (EDX) attachment.

3. Results and discussion

3.1. Sintering process

The densification behavior was studied using the temperature measurement, current and differential effect for samples density during SPS. Figure 1 show densification curves of Ti_3SiC_2 sintered at 1373 K (a) and 1473 K (b) under 30 MPa load for 10 min. The current supplied to punches as a function of

sintering time is also shown in Figure 1. The density function was formed by value changing of sintered samples` calculated density depending on punch displacement values during sintering.

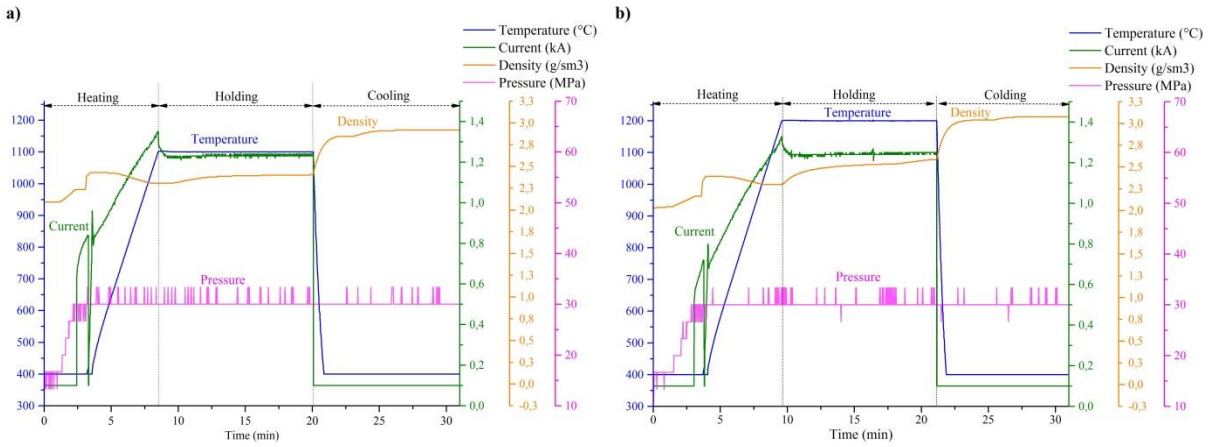

Figure 1. Densification curves of Ti_3SiC_2 sintered at 1373 K (a) and 1473 K (b) under 30 MPa for 10 min.

During spark plasma sintering, the temperature was controlled using a pyrometer. The working temperature range of the pyrometer is 673-3273 K. Therefore, the maximum current is passed through the entire assembly up to 673 K (400 °C) for 3 min heating, then the abrupt behavior of the current values occurs and the current flow is adjusted according to the temperature measurements. In a process of heating (7-10 min) under pressure the density of samples sintered at 1373 K and 1473 K changes in range of (2.1-2.4) g/cm^3. The sharp increase in the density occurs when the electrical current is passing through the moulds. The absorbed gases emitted from surface and volume of the samples and the material is thermally expanded under the heating process. When the temperature reaches 80% from the sintering temperature value, the shrinkage process of the sample is beginning. Nevertheless the density is reduced due to the process of thermal expansion prevails over the shrinkage process.

When the samples are heated to the sintering temperature (isothermal holding), the shrinkage process is the main and the density of the samples sintered at 1373 and 1473 K changes by 0.09 g/cm^3 and 0.28 g/cm^3, respectively.

After isothermal holding, the samples are cooled at a rate of approximately 500 K/min and then pressure is removed after 3-4 minutes. During the entire cooling process, the density of samples sintered at 1373 and 1473 K changes by 0.51 g/cm^3 and 0.49 g/cm^3, respectively. The increasing is caused by the ending of thermal expansion process. The final calculated density of Ti_3SiC_2-based composites sintered at 1373 K and 1473 K are 2.9 g/cm^3 and 3.1 g/cm^3 respectively.

3.2. Phase composition

Figure 2 shows the diffraction patterns of preceramic paper sheet and Ti_3SiC_2-based composites sintered at 1373 K and 1473 K. The results of X-ray analysis show that preceramic paper consist of Ti_3SiC_2, TiC, $TiSi_2$, TiSi crystalline phases and amorphous phase of organic binder. The content of Ti_3SiC_2 in the preceramic paper was more than 90 vol.%. The amorphous phase was not observed after sintering at 1373 K. However, the content of Ti_3SiC_2 phase (60.2 vol.%) significantly decreases along with the growth of TiC (17.3 vol.%), $TiSi_2$ (8.6 vol.%), TiSi (13.9 vol.%) phases. The decrease in the content of Ti_3SiC_2 phase indicates its partly decomposition. Increasing of TiC phase indicates the presence of high amount of carbon which reacts with titanium at 1373 K. Also the decomposition of Ti_3SiC_2 phase is accompanied by increasing of $TiSi_2$ and TiSi content. At the sintering temperature of 1473 K the content of TiC phase increases and the redistribution between $TiSi_2$ and TiSi phases occurs. The content of indicated phases was 22.2, 14.1 and 7.1 vol.%, respectively.

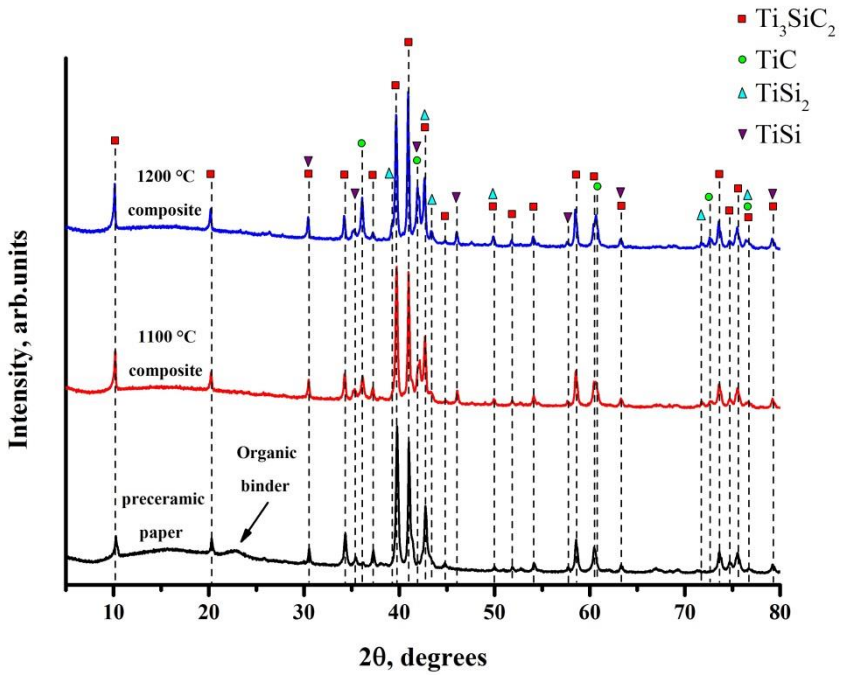

Figure 2. Diffraction patterns of preceramic paper sheet and Ti_3SiC_2-based composites sintered at 1373 K and 1473 K.

3.3. Microstructure and elemental composition

Figure 3 shows the SEM images demonstrating microstructures of the Ti_3SiC_2-based composites sintered at 1373 K (a) and 1473 K (b).

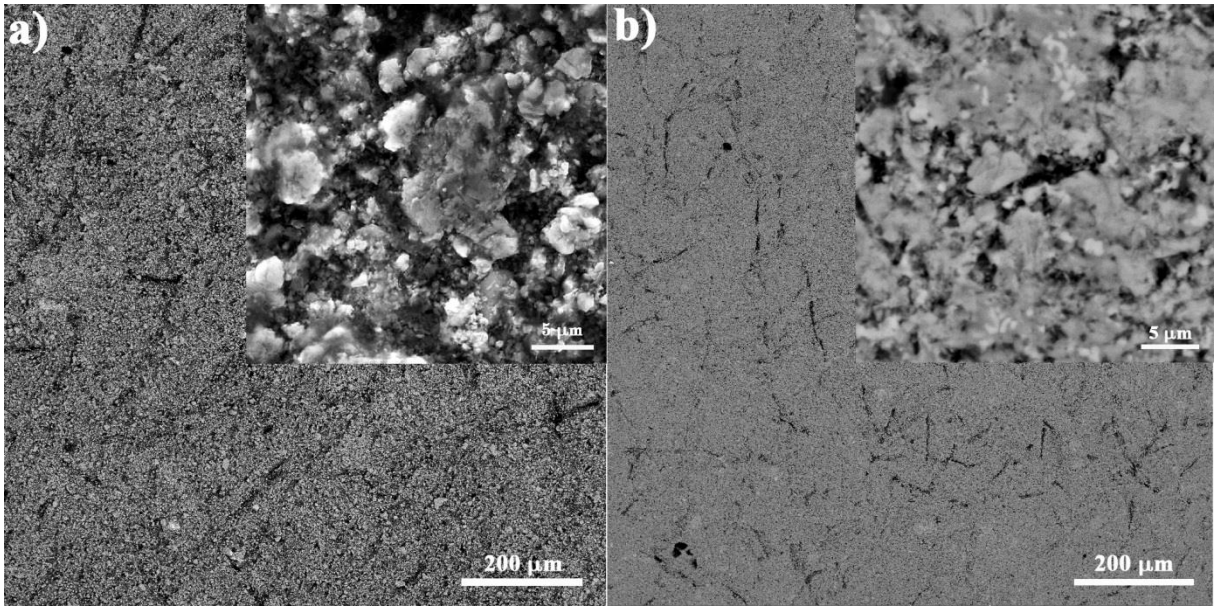

Figure 3. SEM images of Ti_3SiC_2-based composites sintered at 1373 K (a) and 1473 K (b). Insets: higher magnification images.

The analysis of the SEM images shows that microstructure of the sintered composites becomes denser with increasing sintering temperature. Also the traces of cellulose fibers were observed in the composite structure in both cases. Such traces form as the result of decomposition of cellulose fibers

during sintering process. In this case, additional TiC phase can be formed during the reaction between the unbounded carbon from cellulose and the titanium from the Ti_3SiC_2 decomposition reaction. It should be noted that the pore size in the structure of Ti_3SiC_2-based composites sintered at 1473 K does not exceed 2-3 μm. According to EDX analysis the composition of the sintered materials was (44±2) at.% Ti, (23±3) at.% Si and (33±4) at.% C. The results of EDX well correlated with XRD measurements.

4. Conclusion

In this paper the Ti_3SiC_2-based MAX-phase composites were synthesized by spark plasma sintering of preceramic papers at 1373 and 1473 K. The sintered composites consist of multiphase Ti_3SiC_2, TiC, $TiSi_2$, TiSi crystalline structure. The content of Ti_3SiC_2 phase in the sintered at 1373 K composite was 60 vol.%. The partly decomposition of MAX-phase occurs during sintering, and this effect is more pronounced with temperature rise. According to SPS sintering process analysis and scanning electron microscopy, it was established that the microstructure of composite sintered at 1473 K becomes denser. Also the content of TiC and $TiSi_2$ phases increases as well as TiSi phase decreases. The elemental composition of sintered materials was presented by 44 at.% Ti, 23 at.% Si and 33 at.% C, which is well correlate with XRD data. The decomposition of cellulose fibers leads to the formation of specific traces in the structure of spark plasma sintered Ti_3SiC_2-based MAX-phase composites.

Acknowledgements

The work was supported by the Russian Science Foundation (grant No. 19-19-00192).
The authors are grateful to T. Yakich for the SEM analysis.

References

[1] Ying G, He X, Li M, Du S, Han W and He F 2011 *Mater. Sci. Eng*. **528** 2635
[2] Li S B, Yu W B, Zhai H X, Song G M, Sloof W G and Zwaag S 2011 *J. Eur. Ceram. Soc.* **31** 217
[3] Ghosh N C and Harimkar S P 2012 *Consolidation and synthesis of MAX phases by Spark Plasma Sintering (SPS): a review advances in Science and Technology of Mn+1AXn Phases* (Woodhead Publishing) pp 47–80
[4] Zhang Z F 2002 *J. Eur. Ceram. Soc.* **22** 2957
[5] Zhang Z F, Sun Z M and Hashimoto H 2004 *Mater. Sci. Technol.* **20** 1252
[6] Sun Z M 2006 *Scripta Materialia* **55** 1011
[7] Liang B Y, Jin S Z and Wang M Z 2008 *J. Alloys Compd.* **460** 440
[8] Schultheiß J, Dermeik J, Filbert-Demut I, Hock N, Yin N, Greil P and Travitzky N 2015 *Ceram. Intern.* **41** 12595
[9] Lorenz H, Thäter J, Matias Carrijo M M, Rambo C R, Greil P and Travitzky N 2017 *J. Mater. Res.* **32** 3409
[10] Carrijo M. M, Lorenz H, Rambo C. R, Greil P and Travitzky N 2018 *Ceram. Intern*. **44** 8116
[11] Krinitcyn M, Fu Z, Harris J, Kostikov K, Pribytkov G A, Greil P and Travitzky N 2017 Laminated Object Manufacturing of in-situ synthesized MAX-phase composites *Ceram. Intern.* **43** 9241